Chapter 4
Generation of Short and Ultra-Short Pulses

In this chapter we investigate two of the main methods of laser-pulse generation, which are Q-switching and mode-locking. Whilst of-course every laser may be pulsed by just switching it on and off, these methods allow accumulation of pump energy between two pulses, and can therefore, create pulse peak powers that are several orders of magnitude higher than the corresponding cw laser output power.

4.1 Basics of Q-Switching

Q-switching is based on a modulation of the cavity losses, as shown in Fig. 4.1. This modulation, caused by an externally driven intra-cavity modulator in active Q-switching or by a saturable absorber in passive Q-switching, increases the internal losses of the cavity during the pump phase. Thus the laser threshold is dramatically increased and the laser cannot start oscillating, which allows the inversion to reach much higher values than in cw operation. After this pumping phase the modulation losses are switched off and the feedback on the laser medium is restored. Then a laser field builds up from noise and will extract all available stored energy in one giant pulse of high pulse energy. As the loss modulation changes the Q-factor of the cavity, this pulse generation method is called Q-switching. The general temporal evolution of the Q-switch is sketched in Fig. 4.2 for the case of an active Q-switch that acts on the internal cavity losses Λ.

4.1.1 Active Q-Switching

In this section the fundamental properties of actively Q-switched lasers will be deduced, starting from the rate equations (2.60), (2.61).

M. Eichhorn, *Laser Physics*, Graduate Texts in Physics,
DOI 10.1007/978-3-319-05128-4_4,

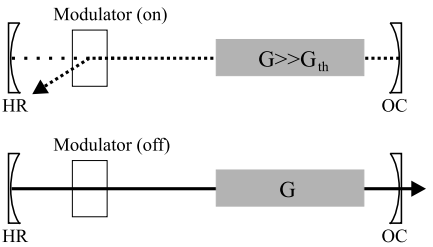

Fig. 4.1 Principle setup of an actively Q-switched laser

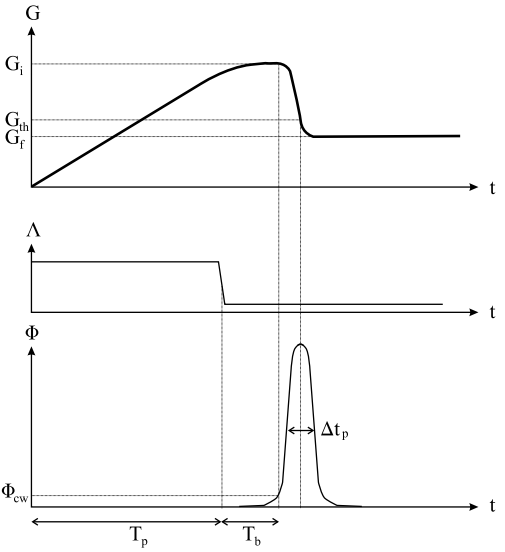

Fig. 4.2 Evolution of gain, loss and photon density during the Q-switch

Pumping at Low Q-Factor

During the pump phase of duration T_p the cavity losses are assumed to be high enough to prevent lasing at all, i.e. $\langle \Phi \rangle \approx 0$. Thus, Eq. (2.60) may be written as

$$\frac{\partial \langle \Delta N \rangle}{\partial t} = R_p - \frac{\langle N \rangle + \langle \Delta N \rangle}{\tau}, \tag{4.1}$$

with the pump rate

$$R_p = 2\frac{\lambda_p}{hc} I_p \frac{\eta_{abs}}{L}. \tag{4.2}$$

This can be easily solved under the assumption of a constant pump rate, resulting in an inversion build-up according to

$$\langle \Delta N \rangle(t) = R_p \tau \left(1 - e^{-\frac{t}{\tau}}\right) - \langle N \rangle. \tag{4.3}$$

It is interesting to note here that this build-up is identical to the charging of a capacitor C, as shown in Fig. 4.3. Q-switching in this sense can thus be seen as slowly

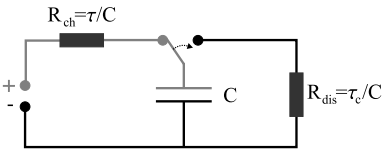

Fig. 4.3 Analogy between Q-switching and the charging of a capacitor

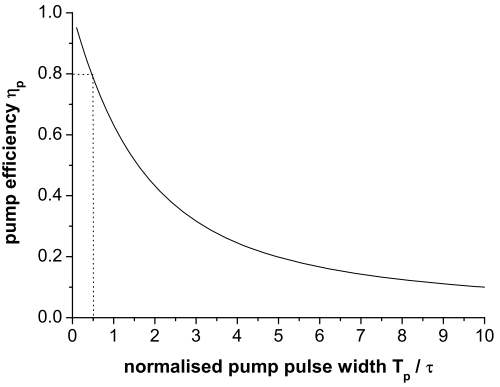

Fig. 4.4 Pump efficiency as a function of the pump pulse width

charging a capacitor over a high resistor $R_{ch} = \frac{\tau}{C}$ and quickly discharging it over a low resistor $R_{dis} = \frac{\tau_c}{C}$, which is connected to the much smaller cavity lifetime.

For a long time pumping, i.e. $t \to \infty$, the inversion will thus saturate and reach its upper limit

$$\langle \Delta N \rangle_\infty = R_p \tau - \langle N \rangle, \tag{4.4}$$

showing that long pumping phases will result in a low efficiency. To calculate the pump efficiency, we assume that the laser is pumped with a given pump energy E_p, which may be distributed over a variable pump time T_p in a square pulse. During this time $N_{p,max} = R_p T_p$ excitations will be created, which however, suffer from spontaneous decay. Therefore, at the end of the pump phase only

$$N_p = \langle \Delta N \rangle (T_p) + \langle N \rangle = \frac{N_{p,max}}{T_p} \tau \left(1 - e^{-\frac{T_p}{\tau}}\right) \tag{4.5}$$

excitations are still in the upper state. Thus the pump efficiency η_p can be derived as

$$\eta_p = \frac{\tau}{T_p} \left(1 - e^{-\frac{T_p}{\tau}}\right), \tag{4.6}$$

giving the amount of absorbed pump energy that is stored inside the laser medium excitation after the pump phase. As can be seen in Fig. 4.4, a pump pulse duration of $T_p < \frac{\tau}{2}$ should be used in order to get a pump efficiency > 80 %.

Pulse Build-Up at High Q-Factor

After the pump phase, the initial inversion $\langle \Delta N \rangle_i$ is present in the laser medium and the modulator is switched off, restoring the high Q-factor of the cavity. We will

now derive the pulse build-up time, which is defined as the time the photon field needs in order to build-up from noise to a value comparable to the photon field in cw operation [1]. As the peak photon density in the Q-switch pulse will be much higher than the cw value $\langle \Phi \rangle_{cw}$, we can assume that for $\langle \Phi \rangle \leq \langle \Phi \rangle_{cw}$ no significant decrease in the inversion occurs. Thus, the inversion is treated as constant during this time, and by using Eq. (2.63), the rate equation governing the temporal evolution of the photon field can be rewritten as

$$\frac{\partial \langle \Phi \rangle}{\partial t} = \frac{c}{2}\big[\sigma_a(\lambda_s) + \sigma_e(\lambda_s)\big]\big(\langle \Delta N \rangle_i - \langle \Delta N \rangle_{th}\big)\langle \Phi \rangle, \tag{4.7}$$

where, we assume that the axial changes in the population and the photon field are not too high, so that we can write the averaged products as the product of the averages. Also, we simplify the cross-sections of absorption and emission at the laser wavelength λ_s by $\sigma_a = \sigma_a(\lambda_s)$ and $\sigma_e = \sigma_e(\lambda_s)$ in the following. Using the abbreviations

$$\langle \Delta N \rangle_i' = \langle \Delta N \rangle_i - \frac{\sigma_a - \sigma_e}{\sigma_a + \sigma_e}\langle N \rangle \tag{4.8}$$

$$\langle \Delta N \rangle_{th}' = \langle \Delta N \rangle_{th} - \frac{\sigma_a - \sigma_e}{\sigma_a + \sigma_e}\langle N \rangle \tag{4.9}$$

$$r = \frac{\langle \Delta N \rangle_i'}{\langle \Delta N \rangle_{th}'} = \frac{g_i}{g_{th}}, \tag{4.10}$$

as well as Eq. (2.63) again we can simplify Eq. (4.7) to the form

$$\frac{\partial \langle \Phi \rangle}{\partial t} = \frac{1}{\tau_c}(r-1)\langle \Phi \rangle, \tag{4.11}$$

with the solution

$$\langle \Phi \rangle(t) = \Phi_0 e^{(r-1)\frac{t}{\tau_c}}, \tag{4.12}$$

where, Φ_0 is the noise photon density caused by the vacuum fluctuations. The cavity field, therefore, will start growing exponentially from the vacuum fluctuations with the time constant $\frac{\tau_c}{r-1}$ until it depletes the inversion significantly. The pump parameter r can also be expressed as the ratio between the initial logarithmic gain g_i and the logarithmic threshold gain g_{th} using

$$g_i = (\sigma_a + \sigma_e)\langle \Delta N \rangle_i - (\sigma_a - \sigma_e)\langle N \rangle \tag{4.13}$$

$$g_{th} = (\sigma_a + \sigma_e)\langle \Delta N \rangle_{th} - (\sigma_a - \sigma_e)\langle N \rangle. \tag{4.14}$$

As long as the depletion of the ground-state N_1 can be neglected during pumping, e.g. in high-repetition rate operation as discussed later on, the logarithmic gain is proportional to the pump power, resulting in

$$r = \frac{g_i}{g_{th}} \approx \frac{P_p}{P_{th}}. \tag{4.15}$$

Therefore, the pump parameter r is often identified with the "times-above-threshold" operation point of the laser given by $r - 1$.

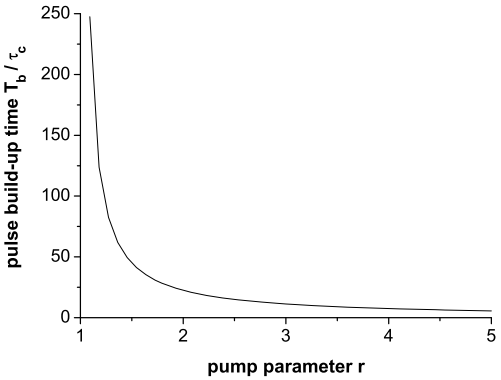

Fig. 4.5 Pulse build-up time as a function of the pump parameter r

Defining the cavity build-up time T_b by $\langle \Phi \rangle (T_b) = \langle \Phi \rangle_{cw}$ results in

$$T_b = \frac{\tau_c}{r-1} \ln \frac{\langle \Phi \rangle_{cw}}{\Phi_0}. \tag{4.16}$$

In most laser systems, the ratio between the cw photon density and the noise is of the order of $10^8 - 10^{12}$, giving

$$T_b \approx (22.5 \pm 5) \frac{\tau_c}{r-1}. \tag{4.17}$$

As shown in Fig. 4.5, the pulse build-up time quickly decreases with increasing pump power, shifting towards the time when the modulator opens. In order not to loose efficiency, additional losses from the modulator must be avoided. Therefore, the modulator has to be chosen so that the switching between the low-Q and the high-Q state of the cavity occurs much faster than the build-up time of the laser pulse.

Pulse Peak Power and Pulse Width

To derive the pulse width of the Q-switch pulse, we can assume that during the pulse build-up and the pulse extraction time, we can neglect further spontaneous decay of the upper level as well as pumping, which results in the rate equations

$$\frac{\partial \langle \Delta N \rangle}{\partial t} = c\big[(\sigma_a - \sigma_e)\langle N \rangle - (\sigma_a + \sigma_e)\langle \Delta N \rangle\big]\langle \Phi \rangle \tag{4.18}$$

$$\frac{\partial \langle \Phi \rangle}{\partial t} = \frac{c}{2}(\sigma_a + \sigma_e)\big(\langle \Delta N \rangle - \langle \Delta N \rangle_{th}\big)\langle \Phi \rangle. \tag{4.19}$$

Dividing Eq. (4.19) by Eq. (4.18) yields the evolution of the photon field with inversion as

$$\frac{\partial \langle \Phi \rangle}{\partial \langle \Delta N \rangle} = \frac{1}{2} \frac{(\sigma_a + \sigma_e)(\langle \Delta N \rangle - \langle \Delta N \rangle_{th})}{(\sigma_a - \sigma_e)\langle N \rangle - (\sigma_a + \sigma_e)\langle \Delta N \rangle}, \tag{4.20}$$

which can be integrated to give the photon field as a function of the inversion density,

$$2\int_{\Phi_0}^{\langle\Phi\rangle} d\langle\Phi\rangle = \int_{\langle\Delta N\rangle_i}^{\langle\Delta N\rangle} \frac{[\sigma_a+\sigma_e](\langle\Delta N\rangle - \langle\Delta N\rangle_{th})}{([\sigma_a-\sigma_e]\langle N\rangle - [\sigma_a+\sigma_e]\langle\Delta N\rangle)} d\langle\Delta N\rangle. \tag{4.21}$$

This integral can be performed analytically and under the assumption that the photon noise density is low compared with the one occurring during the pulse, i.e. we can set the lower integration boundary to $\Phi_0 \approx 0$, this results in

$$\begin{aligned} 2\langle\Phi\rangle \approx{}& \langle\Delta N\rangle_i - \langle\Delta N\rangle \\ &+ \left[\frac{\sigma_a-\sigma_e}{\sigma_a+\sigma_e}\langle N\rangle - \langle\Delta N\rangle_{th}\right] \ln\left(\frac{\langle\Delta N\rangle_i - \frac{\sigma_a-\sigma_e}{\sigma_a+\sigma_e}\langle N\rangle}{\langle\Delta N\rangle - \frac{\sigma_a-\sigma_e}{\sigma_a+\sigma_e}\langle N\rangle}\right). \end{aligned} \tag{4.22}$$

After the pulse is emitted the photon density will decrease to zero again and a residual (final) inversion $\langle\Delta N\rangle_f$ is left inside the medium given by the relation

$$\begin{aligned} &\langle\Delta N\rangle_f - \langle\Delta N\rangle_i \\ &= \left[\frac{\sigma_a-\sigma_e}{\sigma_a+\sigma_e}\langle N\rangle - \langle\Delta N\rangle_{th}\right] \ln\left(\frac{\langle\Delta N\rangle_i - \frac{\sigma_a-\sigma_e}{\sigma_a+\sigma_e}\langle N\rangle}{\langle\Delta N\rangle_f - \frac{\sigma_a-\sigma_e}{\sigma_a+\sigma_e}\langle N\rangle}\right). \end{aligned} \tag{4.23}$$

This is the main equation describing the Q-switch process. Using the abbreviations in Eqs. (4.8)–(4.10) and accordingly

$$\langle\Delta N\rangle'_f = \langle\Delta N\rangle_f - \frac{\sigma_a-\sigma_e}{\sigma_a+\sigma_e}\langle N\rangle \tag{4.24}$$

the fundamental Q-switch equation can be rewritten in the simple form

$$\frac{\langle\Delta N\rangle'_f}{\langle\Delta N\rangle'_i} = 1 - \frac{1}{r}\ln\frac{\langle\Delta N\rangle'_i}{\langle\Delta N\rangle'_f}, \tag{4.25}$$

showing that the whole Q-switch pulse evolution only depends on the initial inversion $\langle\Delta N\rangle'_i$ and the cavity parameters included in $\langle\Delta N\rangle'_{th}$.

To derive the pulse peak power, we first have to find the time of the pulse peak itself. As already shown in Fig. 4.2, the peak is reached when no further net amplification is possible, i.e. it will occur exactly when the gain, and thus the inversion, crosses the threshold values. Using Eq. (4.22) thus gives the peak photon density inside the cavity as

$$\langle\hat{\Phi}\rangle = \frac{r-1-\ln r}{2}\langle\Delta N\rangle'_{th}. \tag{4.26}$$

Therefore, it only depends on the cavity parameters and r. As these photons will leave the cavity with the cavity photon lifetime τ_c, the peak power of the Q-switched pulse can be directly given by

$$\hat{P} = \frac{h\nu}{\tau_c}\langle\hat{\Phi}\rangle V = \frac{r-1-\ln r}{2}\langle\Delta N\rangle'_{th}\frac{h\nu}{\tau_c}V. \tag{4.27}$$

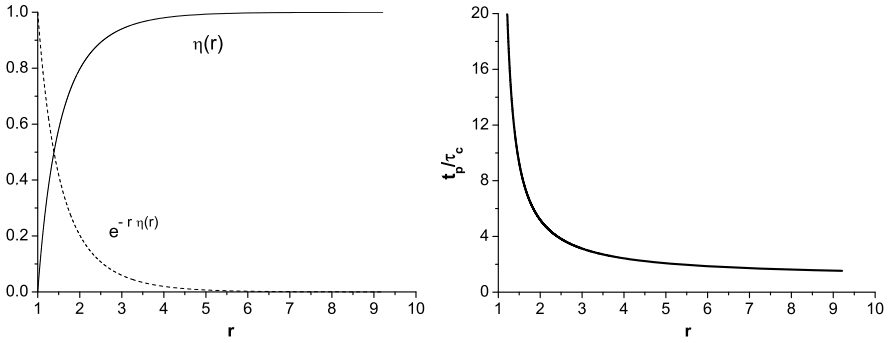

Fig. 4.6 Extraction efficiency and relative pulse width of a Q-switch pulse as a function of the pump parameter r

Additionally, we define the energy extraction efficiency η_e by the fraction of extracted inversion as

$$\eta_e = 1 - \frac{\langle \Delta N \rangle'_f}{\langle \Delta N \rangle'_i}. \tag{4.28}$$

Using Eq. (4.25) the energy extraction efficiency $\eta_e(r)$ can be calculated independently from the actual laser parameters by the transcendental equation

$$r = -\frac{\ln[1 - \eta_e(r)]}{\eta_e(r)}. \tag{4.29}$$

Hence, we can approximate the pulse width t_p of the Q-switch pulse as the ratio between the extracted energy $E_s = \frac{1}{2} h\nu V(\langle \Delta N \rangle'_i - \langle \Delta N \rangle'_f)$ and the pulse peak power $\hat{P}$ by

$$t_p \approx \frac{E_s}{\hat{P}} = \frac{r\eta_e(r)}{r - 1 - \ln r}\tau_c. \tag{4.30}$$

The factor $\frac{1}{2}$ in the energy takes into account that in the ΔN each excitation is counted twice.

As can be seen in Fig. 4.6 the extraction efficiency quickly approaches unity for $r > 4$, whilst the pulse width asymptotically decreases towards the cavity lifetime. This shows that short pulses on the order on several ns to 1 µs are possible with Q-switched lasers, depending on the cavity lengths and lifetimes.

4.1.2 Experimental Realization

Q-switching is most often achieved through use of two main techniques, in which either an acousto-optic modulator (AOM) or an electro-optic modulator (EOM) is used to modify the cavity losses. The initial technique was to rotate the HR mirror of the cavity around an axis perpendicular to the beam propagation axis. This

generates a Q-switch pulse, because only during the short time when the mirror is perpendicularly aligned to the beam, a high-Q cavity is formed. A special pulse-generation method is cavity dumping, in which the laser is Q-switched between two HR mirrors. Then the pulse builds up and is finally extracted by using the modulator a second time. This last technique usually needs fast switching times as especially the switching to extract the pulse has to be much faster than the cavity round-trip time. Therefore, only electro-optical modulators are used in this case.

Acousto-Optic Modulators

The usual setup of an acousto-optically Q-switched laser is shown in Fig. 4.7. The modulator consists of a transparent material, e.g. silica glass (SiO_2) or tellurium dioxide (TeO_2), to which an ultrasonic transducer is bonded to create a sound wave inside the bulk modulator material. Owing to the photo-elastic effect, this sound wave generates an index of refraction distribution inside the modulator material, which behaves as an optical phase grating that causes a part of the incident power to be diffracted out of the cavity, thus creating losses. By switching off the radio-frequency (rf) power to the transducer, the glass block returns to its homogeneous index state and the high Q-factor of the resonator is restored [3].

Depending on the length L_m of the modulator material, the wavelengths of the optical wave and the sound wave, two diffraction regimes are observed, which are the Raman-Nath regime and the Bragg regime.

In **Raman-Nath scattering** the interaction length L_m is short or the sound wavelength λ_a is large, thus $\lambda_s L_m \ll \lambda_a^2$. In this case, the incident light is scattered into many diffraction orders, with a maximum of diffracted power occurring when the sound wave interacts perpendicularly with the light wave, as shown in Fig. 4.8. The amplitude of the phase grating is given by

$$\Delta\phi = 2\pi\,\Delta n \frac{L_m}{\lambda_s} = \pi \sqrt{\frac{2L_m}{\lambda_s^2} M_2 \frac{P_a}{b}}, \tag{4.31}$$

with b being the width of the sound wave, P_a the acoustic wave power and M_2 the so-called figure of merit of the acousto-optic material. It can be calculated from the refractive index n, the photoelastic coefficient in the chosen geometry p, the density of the acousto-optic material ρ and the velocity of sound v_a as

$$M_2 = \frac{n^6 p^2}{\rho v_a^3}. \tag{4.32}$$

Finally, the intensity scattered into the nth order is given by

$$I_n = \hat{I}_0 J_n^2(\Delta\phi), \tag{4.33}$$

where, $J_n(x)$ is the Bessel function of nth order and $\hat{I}_0$ the incident laser intensity.

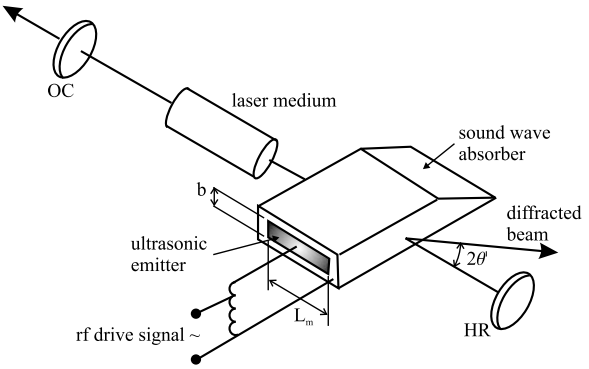

Fig. 4.7 Setup of an actively Q-switched laser using an acousto-optic modulator [3]

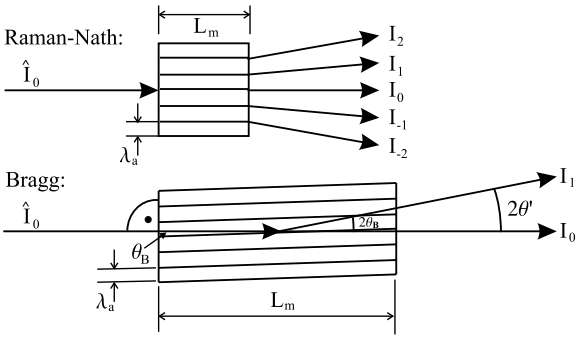

Fig. 4.8 The two operation regimes of an acousto-optic modulator: The Raman-Nath regime and the Bragg regime [3]

In **Bragg scattering**, described by $\lambda_s L_m \gg \lambda_a^2$, a zero-order and first-order diffraction beam become predominant under the Bragg condition [3], in this case the sound wave and the light wave interact at the **Bragg angle** θ_B, given by

$$\sin\theta_B = \frac{\lambda_s}{2n\lambda_a}. \tag{4.34}$$

The internal deflection angle is given by $2\theta_B$ and by taking into account the refraction on the output side of the modulator, one finds an external diffraction angle of

$$\theta' = 2n\theta_B \approx \frac{\lambda_s}{\lambda_a}. \tag{4.35}$$

The intensity of the scattered beam is then given by

$$I_1 = \hat{I}_0 \sin^2 \frac{\Delta\phi}{2}, \tag{4.36}$$

and the intensity of the transmitted beam I_0 is reduced by this amount compared with the off-state of the modulator.

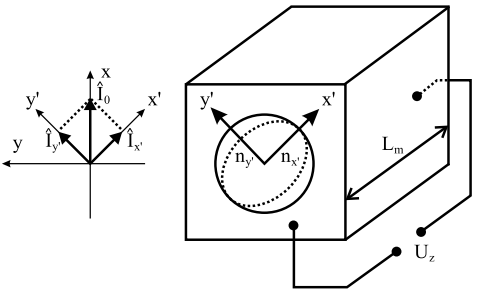

Fig. 4.9 Layout of a Pockels cell as an electro-optic modulator and the induced change in the refractive index ellipsoid [3]

Electro-Optic Modulators

Whilst acousto-optic modulators may also be used with unpolarized light, an electro-optic modulator uses the electro-optic effect, i.e. the birefringence induced in an optical medium by an externally applied electric field. This is achieved in a **Pockels cell**, in which the refractive index change depends linearly on the applied electric field (**Pockels effect**). The external electric field will induce a birefringence, which results in a so-called slow-axis and a fast-axis with different indices of refraction. The electro-optic crystal, e.g. potassium dihydrogen phosphate (KDP), is oriented in such way that the incident laser light will have its polarized aligned under 45° with respect to the slow or fast axis, see Fig. 4.9. Then, the induced change in refractive index will cause a phase shift between the slow- and fast-axis electric field components of the beam. This results in a change of the state of polarization of the radiation, developing from an incident linear polarization to an elliptical polarization and a circular polarization during its propagation along the cell axis.

For a given cell length L_c two specific voltages exist for which the output polarization corresponds to a circular polarization or a linear polarization rotated by 90° with respect to the incident polarization orientation. These voltages are called quarter-wave $U_{\frac{\lambda}{4}}$ and half-wave voltage $U_{\frac{\lambda}{2}}$, respectively,

$$U_{\frac{\lambda}{4}} = \frac{\lambda_s}{4n_0^3 r_{63}}, \tag{4.37}$$

$$U_{\frac{\lambda}{2}} = \frac{\lambda_s}{2n_0^3 r_{63}}, \tag{4.38}$$

as the cell acts like a quarter- or half-wave plate in this case. In this formulae, wherein n_0 is the ordinary index of refraction, λ_s is the laser wavelength and r_{63} is the electro-optic coefficient. Combining such a Pockels cell with an intracavity polarizer now allows efficient and fast switching of the internal beam as the electro-optic effect has a response time much smaller than the cavity time constants. The switching time only depends on the high-voltage power supply and its ability to charge the Pockels cell, which is electrically charged just like a capacitor.

The quarter-wave setup only needs one intra-cavity polarizer, since the beam passes the Pockels cell twice resulting in a total polarization rotation of 90° as shown in Fig. 4.10. In the half-wave setup a second polarizer is needed to couple out the

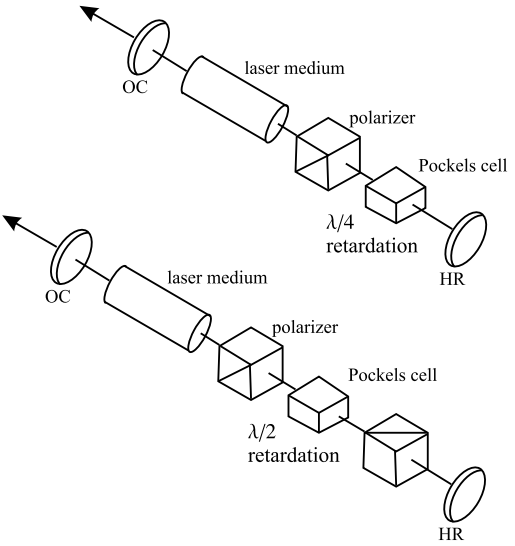

Fig. 4.10 Setup of an actively Q-switched laser using an electro-optic modulator [3]

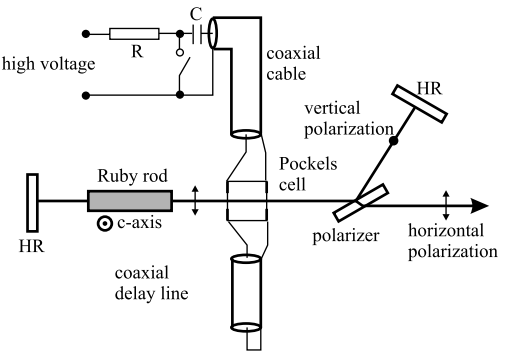

Fig. 4.11 Setup of a cavity-dumped ruby laser [3]

all the incident radiation when the voltage is applied. By switching off the voltage in both cases the electro-optic crystal will return into its non-birefringent state and the cavity is restored, causing the Q-switch pulse to build up.

Cavity Dumping

In cavity dumping the half-wave setup of a Pockels cell is used and the laser is Q-switched with nearly 100 % reflectivity cavity mirrors in order to obtain very short Q-switch pulses. At the peak of the Q-switched pulse, the Pockels cell is used to switch the closed cavity rapidly to its output port, provided by an intracavity polarizer. Thus, the width of the Q-switched pulse is only a function of the cavity length and its round-trip time, and not of the spectroscopic parameters of the laser medium. In the example in Fig. 4.11 the ruby laser rod is oriented so that the c-axis is

perpendicular to the plane of the page. Without any voltage on the Pockels cell, the laser medium is pumped and an inversion is created. The crystal only provides a high optical gain for a laser polarization in this plane, so that the generated fluorescence does not "see" the second cavity mirror as it leaves the cavity by passing through the polarizer. Then the half-wave voltage is applied to the Pockels cell, causing the polarized fluorescence to be reflected from the polarizer. Hence, the laser cavity is closed and the laser pulse builds up. On the maximum laser pulse power, the voltage is removed from the Pockels cell in less than 2–5 ns and the cavity photons will all leak out by passing the polarizer, thus creating a pulse with a width of the round-trip time of the resonator.

If the laser medium does not provide a polarized output itself, a second polarizer can be inserted into the cavity to provide the decoupling of the second cavity mirror during the off-state of the Pockels cell.

4.1.3 Passive Q-Switching

In contrast to active Q-switching, where an external signal is applied to open the cavity and to restore the high Q-factor to generate the pulse, passive Q-switching uses a **saturable absorber**. This is an additional medium inside the cavity that absorbs on the laser wavelength, thus decreasing the Q-factor (or increasing the internal cavity losses). However, this absorption is intensity dependent and quickly saturates towards a highly transmissive state of that material, restoring the high Q-factor of the cavity, which causes the build-up of the pulse intensity. This switching can be seen in Fig. 4.12, in which the transmission of a saturable medium is shown with respect to the incident fluence

$$J = \int I_s dt \tag{4.39}$$

on the absorption line. By analogy with the Frantz-Nodvik model [2], this transmission can be calculated by

$$T(J) = \frac{J_{sat}}{J} \ln\left[1 + \left(e^{\frac{J}{J_{sat}}} - 1\right) T_0\right], \tag{4.40}$$

where, T_0 is the initial, i.e. unpumped, transmission of the saturable medium and J_{sat} is the saturation fluence, given by

$$J_{sat} = \frac{hc}{\lambda_s[\sigma_a(\lambda_s) + \sigma_e(\lambda_s)]} = \tau^* I^s_{sat}, \tag{4.41}$$

with τ^* being the excitation lifetime of the saturable absorber and

$$I^s_{sat} = \frac{hc}{\lambda_s[\sigma_a(\lambda_s) + \sigma_e(\lambda_s)]\tau^*} \tag{4.42}$$

being the saturation intensity of the absorber on the laser line. It should not be confused with the pump saturation intensity in Eq. (2.71), in which the pump wavelength λ_p occurs.

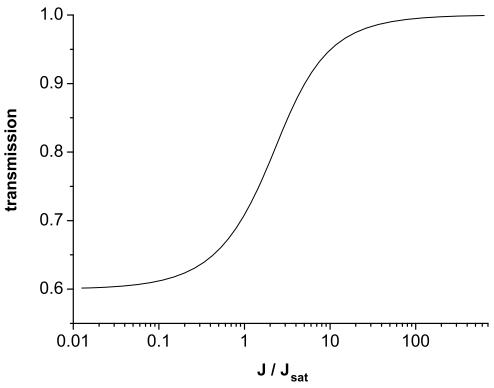

Fig. 4.12 Transmission of a saturable medium as a function of the incident fluence at an initial transmission of $T_0 = 0.6$

Owing to the additional saturable absorber inside the cavity, a new rate equation has to be added to describe this system. The passive Q-switch on the time scale of the pulse generation, i.e. when pumping and spontaneous decay can be neglected, is therefore given by the coupled equations

$$\frac{\partial\langle\Delta N\rangle}{\partial t} = c\big[(\sigma_a - \sigma_e)\langle N\rangle - (\sigma_a + \sigma_e)\langle\Delta N\rangle\big]\langle\Phi\rangle \tag{4.43}$$

$$\frac{\partial\Delta N^*}{\partial t} = c\big[\big(\sigma_a^* - \sigma_e^*\big)N^* - \big(\sigma_a^* + \sigma_e^*\big)\Delta N^*\big]\langle\Phi\rangle - \frac{\Delta N^* + N^*}{\tau^*} \tag{4.44}$$

$$\begin{aligned}\frac{\partial\langle\Phi\rangle}{\partial t} &= \frac{c}{2}(\sigma_a + \sigma_e)\big(\langle\Delta N\rangle - \langle\Delta N\rangle_{th}\big)\langle\Phi\rangle \\ &\quad + \frac{c}{2}\big[\big(\sigma_a^* + \sigma_e^*\big)\Delta N^* - \big(\sigma_a^* - \sigma_e^*\big)N^*\big]\langle\Phi\rangle,\end{aligned} \tag{4.45}$$

where, ΔN^* and N^* are the inversion density and total absorber density of the saturable absorber, τ^* its excitation lifetime and $\sigma_a^* = \sigma_a^*(\lambda_s)$ and $\sigma_e^* = \sigma_e^*(\lambda_s)$ the saturable absorber cross-sections of absorption and emission at the laser wavelength λ_s.

A saturable absorber usually has a very low excitation lifetime $\tau^* <$ ns, much lower than the Q-switch pulse widths created. It often uses dyes or semiconductor materials. Thus, the inversion density of the saturable absorber ΔN^* in Eq. (4.44) will nearly instantaneously react on the photon density $\langle\Phi\rangle$. Therefore, we can approximately solve this rate equation as being in the steady state compared to all other processes during the Q-switch. This results in

$$\Delta N^* = \frac{c\tau^*(\sigma_a^* - \sigma_e^*)\langle\Phi\rangle - 1}{c\tau^*(\sigma_a^* + \sigma_e^*)\langle\Phi\rangle + 1}N^*. \tag{4.46}$$

At the beginning of the Q-switch process, it can be assumed that the laser medium has its initial inversion density $\langle\Delta N\rangle_i$ and that the saturable absorber is still unexcited, i.e. $\Delta N^* \approx -N^*$. Therefore, Eq. (4.45) gives

$$\frac{\partial\langle\Phi\rangle}{\partial t} = \frac{c}{2}(\sigma_a + \sigma_e)\big(\langle\Delta N\rangle_i - \langle\Delta N\rangle_{th}\big)\langle\Phi\rangle - c\sigma_a^* N^*\langle\Phi\rangle, \tag{4.47}$$

which results in an exponentially growing photon field $\langle \Phi \rangle(t) = \Phi_0 e^{\gamma_0 t}$ with a time constant

$$\gamma_0 = \frac{c}{2}(\sigma_a + \sigma_e)\big(\langle \Delta N \rangle_i - \langle \Delta N \rangle_{th}\big) - c\sigma_a^* N^*. \tag{4.48}$$

In contrast to the temporal behaviour of the saturable absorber inversion density, the inversion density $\langle \Delta N \rangle(t)$ of the laser medium will be determined by the integrated photon flux. By taking the approximate exponential growth solution of Eq. (4.47), and the analytical solution of

$$\frac{\partial f}{\partial t} = \big(af(t) + b\big)u(t), \tag{4.49}$$

given by

$$f(t) = e^{a\int_0^t u(t')dt'}\left(f(0) + b\int_0^t e^{-a\int_0^{t'} u(t'')dt''} u\big(t'\big)dt'\right), \tag{4.50}$$

Eq. (4.43) can be analytically solved, giving

$$\langle \Delta N \rangle = e^{-\frac{c(\sigma_a+\sigma_e)}{\gamma_0}\langle \Phi \rangle(t)}\left(\langle \Delta N \rangle_i + c(\sigma_a - \sigma_e)\langle N \rangle \int_0^t e^{\frac{c(\sigma_a+\sigma_e)}{\gamma_0}\langle \Phi \rangle(t')} \langle \Phi \rangle\big(t'\big)dt'\right). \tag{4.51}$$

Inserting these results into Eq. (4.45), the exponential time constant of the photon field can be described by

$$\frac{1}{\langle \Phi \rangle}\frac{\partial \langle \Phi \rangle}{\partial t} = \gamma_0 + \left(c^2\sigma_a^*\big(\sigma_a^* + \sigma_e^*\big)\tau^* N^* - \frac{c^2(\sigma_a + \sigma_e)^2}{2\gamma_0}\langle \Delta N \rangle_i\right)\langle \Phi \rangle + \cdots, \tag{4.52}$$

wherein a series development in the power of $\langle \Phi \rangle$ was used.

If the coefficient of the linear term in $\langle \Phi \rangle$ has a negative sign, the exponential time constant will decrease with increasing photon flux, which means that the gain provided by the laser medium saturates before the absober can saturate. This will thus not result in a Q-switch pulse. However, when the sign of this linear term is positive, the exponential time constant will increase with increasing photon flux as the saturable absorber bleaches much faster than the gain of the laser medium is reduced owing to amplification. Then, a Q-switch pulse is emitted as shown in Fig. 4.13. Passive Q-switching thus depends on two thresholds: a first threshold that needs to be passed by pumping strongly enough that the generated gain exceeds the unsaturated losses of the cavity including the saturable absorber, and a second threshold that is given by passing the point after which the photon flux grows faster than exponentially. If we denote the single-pass gain before saturation occurs with G_0, the logarithmic round-trip gain results in $g_0 = 2\ln G_0$. Hence, the exponential time constant γ_0 may be approximated by

$$\gamma_0 \approx \frac{g_0}{\Delta t_{RT}}, \tag{4.53}$$

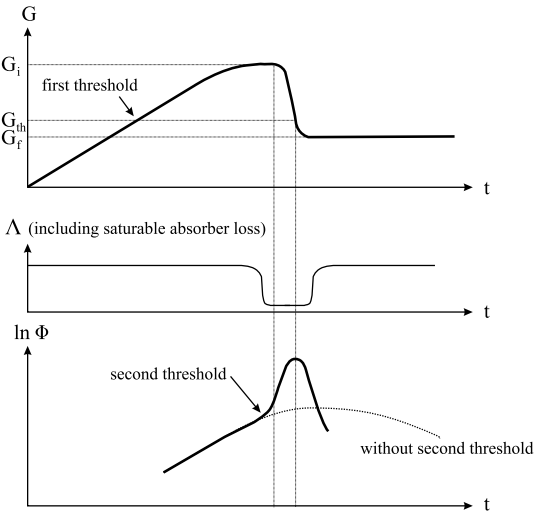

Fig. 4.13 Evolution of gain, loss and photon density during the passive Q-switch

neglecting the cavity photon lifetime, see Eq. (2.62). Therein, Δt_{RT} is the cavity round-trip time. Then, the **second threshold** can be expressed by

$$N^* > \frac{(\sigma_a + \sigma_e)^2}{\sigma_a^*(\sigma_a^* + \sigma_e^*)} \frac{\Delta t_{RT}}{\tau^*} \frac{\langle \Delta N \rangle_i}{2g_0}, \tag{4.54}$$

stating the minimum absorber density necessary to pass the second threshold.

4.1.4 Scaling Laws of Repetitive Q-Switching

In this section we will investigate repetitive Q-switching, i.e. a periodic opening and closing of the cavity by the modulator at a repetition rate ν_{Rep} and with an opening time t_G, called a gate. Of-course, the gate t_G has to be at least as long as the pulse build-up time. As a result from the finite pulse build-up time an upper limit will exist for the repetition rate, given by the fact that during the corresponding repetition period $T_{Rep} = \frac{1}{\nu_{Rep}}$ enough inversion, and thus, gain has to build-up so that the pulse will be created within the gate duration, i.e. during the high-Q state of the cavity.

In repetitive Q-switching under equilibrium conditions, i.e. when all pulses show equal pulse energy, it follows from the dependence of the Q-switch pulse evolution in Eq. (4.25) that the initial inversion before each pulse emission has to be equal. As the initial inversion of the nth pulse is coupled to the final inversion of the $n-1^{th}$ pulse, by the pumping between the two pulses, we can conclude from self-consistency, using Eq. (4.1), that

$$\begin{aligned} \langle \Delta N \rangle_i &= \left(\langle \Delta N \rangle_f - R_p \tau + \langle N \rangle \right) e^{-\frac{T_{Rep}}{\tau}} + R_p \tau - \langle N \rangle \\ &= \langle \Delta N \rangle_\infty - \left(\langle \Delta N \rangle_\infty - \langle \Delta N \rangle_f \right) e^{-\frac{1}{\nu_{Rep} \tau}}. \end{aligned} \tag{4.55}$$

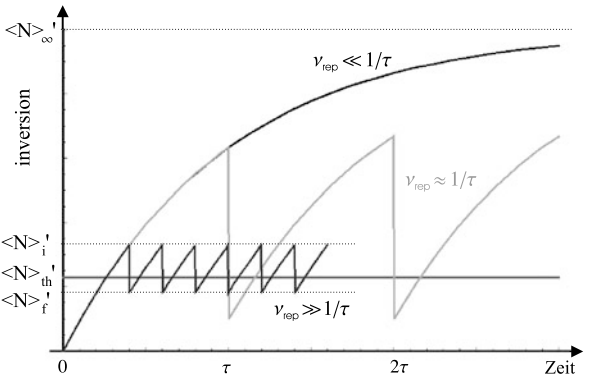

Fig. 4.14 Evolution of the inversion with time for high-repetition-rate Q-switching

Using the abbreviations in Eqs. (4.8)–(4.10), (4.24) and accordingly

$$\langle \Delta N \rangle'_\infty = \langle \Delta N \rangle_\infty - \frac{\sigma_a - \sigma_e}{\sigma_a + \sigma_e} \langle N \rangle, \tag{4.56}$$

Eq. (4.55) can be rewritten to

$$\langle \Delta N \rangle'_i = \langle \Delta N \rangle'_\infty - \left(\langle \Delta N \rangle'_\infty - \langle \Delta N \rangle'_f \right) e^{-\frac{1}{\nu_{Rep}\tau}}. \tag{4.57}$$

The other two equations necessary to derive the scaling laws are rewritten forms of Eqs. (4.25), (4.30) and are given by

$$\langle \Delta N \rangle'_i - \langle \Delta N \rangle'_f = \langle \Delta N \rangle'_{th} \ln \frac{\langle \Delta N \rangle'_i}{\langle \Delta N \rangle'_f}, \tag{4.58}$$

$$\Delta t_p = \frac{\langle \Delta N \rangle'_i - \langle \Delta N \rangle'_f}{\langle \Delta N \rangle'_i - \langle \Delta N \rangle'_{th} (1 + \ln \frac{\langle \Delta N \rangle'_i}{\langle \Delta N \rangle'_{th}})} \tau_c. \tag{4.59}$$

In the case of low repetition rates, i.e. $\nu_{Rep} \ll \frac{1}{\tau}$, Eq. (4.57) yields $\langle \Delta N \rangle'_i \approx \langle \Delta N \rangle'_\infty$ and thus, using Eq. (4.58), that $\langle \Delta N \rangle'_f \approx$ constant. Therefore, also the pulse width Δt_p, pulse peak power $\hat{P}$ and pulse energy E_s are constant and the average power, given by

$$\langle P_s \rangle = \frac{1}{2} h\nu V \left(\langle \Delta N \rangle'_i - \langle \Delta N \rangle'_f \right) \nu_{Rep}, \tag{4.60}$$

scales with the repetition rate.

For high repetition rates, i.e. $\nu_{Rep} \gg \frac{1}{\tau}$, this calculation is a little bit more complex. In this case, we can assume $\langle \Delta N \rangle'_i \approx \langle \Delta N \rangle'_f$, as shown in Fig. 4.14, and we can thus develop the logarithm in Eq. (4.58) to third order,

$$\ln x \simeq -\frac{(x-1)^2}{2} + x - 1, \tag{4.61}$$

resulting in

$$\frac{\langle \Delta N \rangle'_f}{\langle \Delta N \rangle'_{th}} \simeq 2 - \frac{\langle \Delta N \rangle'_i}{\langle \Delta N \rangle'_f}. \tag{4.62}$$

Table 4.1 Scaling laws of the repetitively Q-switched laser

Repetition rate	Average power	Pulse width	Peak power	Pulse energy
$\nu_{Rep} \ll \frac{1}{\tau}$	$\langle P_s \rangle \propto \nu_{Rep}$	$\Delta t \sim \text{const}$	$\hat{P} \sim \text{const}$	$E_s \sim \text{const}$
$\nu_{Rep} \gg \frac{1}{\tau}$	$\langle P_s \rangle \sim \text{const}$	$\Delta t \propto \nu_{Rep}$	$\hat{P} \propto \frac{1}{\nu_{Rep}^2}$	$E_s \propto \frac{1}{\nu_{Rep}}$

As we can also assume $\langle \Delta N \rangle_i' \approx \langle \Delta N \rangle_{th}'$, we can use the same third-order development in Eq. (4.59) and insert the result of Eq. (4.62), giving

$$\Delta t_p \simeq \tau_c \frac{\langle \Delta N \rangle_i' - \langle \Delta N \rangle_f'}{\frac{\langle \Delta N \rangle_{th}'}{2} (1 - \frac{\langle \Delta N \rangle_i'}{\langle \Delta N \rangle_f'})^2}. \tag{4.63}$$

Using the equivalent of Eq. (4.58),

$$\frac{\langle \Delta N \rangle_i'}{\langle \Delta N \rangle_f'} = e^{\frac{\langle \Delta N \rangle_i' - \langle \Delta N \rangle_f'}{\langle \Delta N \rangle_{th}'}} \simeq 1 + \frac{\langle \Delta N \rangle_i' - \langle \Delta N \rangle_f'}{\langle \Delta N \rangle_{th}'} \tag{4.64}$$

for $\frac{\langle \Delta N \rangle_i' - \langle \Delta N \rangle_f'}{\langle \Delta N \rangle_{th}'} \ll 1$, we can deduce

$$\Delta t_p \simeq \frac{2\tau_c \langle \Delta N \rangle_{th}'}{\langle \Delta N \rangle_i' - \langle \Delta N \rangle_f'}. \tag{4.65}$$

As $\nu_{Rep} \gg \frac{1}{\tau}$, it follows from Eq. (4.57) that

$$\langle \Delta N \rangle_i' - \langle \Delta N \rangle_f' \simeq \frac{\langle \Delta N \rangle_\infty' - \langle \Delta N \rangle_f'}{\tau \nu_{Rep}}, \tag{4.66}$$

and from $\langle \Delta N \rangle_f' \ll \langle \Delta N \rangle_\infty'$ we finally obtain

$$\Delta t_p \propto \frac{\nu_{Rep}}{\langle \Delta N \rangle_\infty'}. \tag{4.67}$$

Thus, the pulse width will increase linearly with repetition rate for a constant pump power, and it will decrease with increasing pump power, i.e. with increasing $\langle \Delta N \rangle_\infty'$. Using Eq. (4.60) and the relation

$$\hat{P} = \frac{\langle P_s \rangle}{\Delta t_p \nu_{Rep}} \tag{4.68}$$

we obtain the other scaling laws shown in Table 4.1.

As for high repetition rates, the average output power is constant; this regime of operation is also often called **quasi-continuous operation**. Resulting from the linear increase in pulse width, as well as the fact that with increasing repetition rate, the pulse energy is distributed over an increasing number of pulses, the peak power will strongly decrease with the inverse square of the repetition rate. For low repetition rate operation, the continuous pumping will saturate the inversion and the initial inversion becomes pump duration, i.e. repetition period, independent. Therefore, every pulse has the maximum pulse energy given by the completely inverted

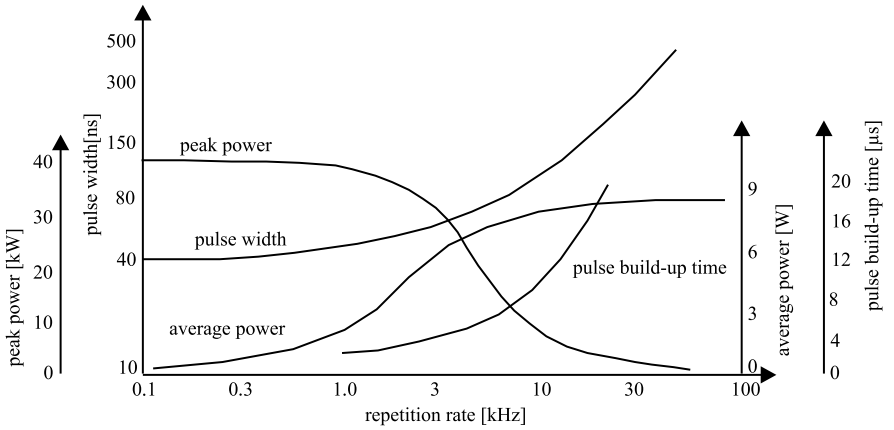

Fig. 4.15 Evolution of the laser output parameters with repetition rate for a continuously-pumped Q-switched laser [3]

population in the laser medium and the average output power simply increases with repetition rate. However, it has to be noted here that this case is usually difficult to achieve. In most lasers the fully inverted laser medium corresponds to such a high pulse energy that the optical damage threshold of the coatings on some intracavity components, such as the mirrors or the laser medium itself will be exceeded, resulting in the destruction of this component. The transition between the two repetition frequency regimes is non-linear and makes a numerical solution of the rate equations necessary. In summary, the dependence of the output parameters of a continuously-pumped Q-switched Nd^{3+}:YVO_4 laser is shown in Fig. 4.15.

4.2 Basics of Mode Locking and Ultra-Short Pulses

As we investigated in the previous chapter, short laser pulses on the order of the cavity lifetime τ_c, i.e. with a duration of several ns to µs, can be created with the Q-switch technique. In a careful design the laser, these pulses may correspond to a single longitudinal mode. If much shorter pulses are necessary, the longitudinal mode structure of the laser needs to be exploited, as pulse width and laser spectrum are coupled by an uncertainty-like relation. To investigate this, we consider a Gaussian laser pulse with an electric field amplitude

$$E(t) = E_0 e^{-\xi t^2} e^{i\omega_0 t} \tag{4.69}$$

with a Gaussian parameter

$$\xi = a - ib. \tag{4.70}$$

Thus, the laser pulse intensity $I(t) \propto |E(t)|^2$ will be

$$I(t) = I_0 e^{-4\ln 2(\frac{t}{\tau_p})^2}, \tag{4.71}$$

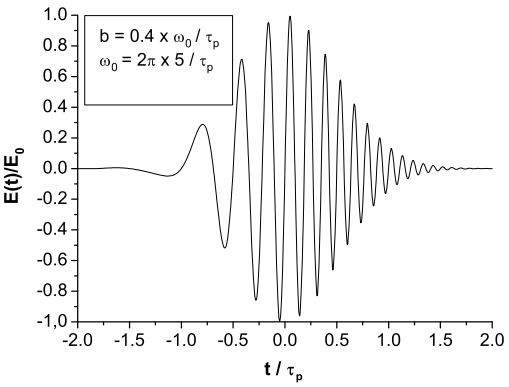

Fig. 4.16 Electric field of a chirped Gaussian pulse

where, the pulse width τ_p is given by

$$\tau_p = \sqrt{\frac{2\ln 2}{a}}. \tag{4.72}$$

We can interpret $a = \Re(\xi)$ as being connected to the pulse width, while $b = \Im(\xi)$ is connected to the **chirp** of the pulse, i.e. the time-dependent frequency shift during the pulse. This can be seen directly from Eq. (4.69), which results in a total pulse phase given by

$$\phi = \omega_0 t + bt^2, \tag{4.73}$$

so that the actual laser frequency is given by

$$\omega = \frac{\partial \phi}{\partial t} = \omega_0 + 2bt. \tag{4.74}$$

Therefore, b describes a linear chirp, i.e. a linearly increasing laser frequency during the pulse, as shown in Fig. 4.16.

In order to derive the relation between laser pulse width and the spectral output, the frequency spectrum of the electric field is calculated by its Fourier transform,

$$\tilde{E}(\omega) = \tilde{E}_0 e^{-\frac{(\omega-\omega_0)^2}{4\xi}} = \tilde{E}_0 e^{-\frac{1}{4}\left(\frac{a}{a^2+b^2}+i\frac{b}{a^2+b^2}\right)(\omega-\omega_0)^2}. \tag{4.75}$$

Therefore, the spectral intensity distribution $\tilde{I}(\omega) \propto |\tilde{E}(\omega)|^2$ is given by

$$\tilde{I}(\omega) = \tilde{I}_0 e^{-\frac{1}{2}\frac{a}{a^2+b^2}(\omega-\omega_0)^2} = \tilde{I}_0 e^{-4\ln 2\left(\frac{\omega-\omega_0}{2\pi\Delta\nu_p}\right)^2}. \tag{4.76}$$

Thus, the pulse bandwidth results in

$$\Delta\nu_p = \frac{\sqrt{2\ln 2}}{\pi}\sqrt{a\left(1+\left(\frac{b}{a}\right)^2\right)}, \tag{4.77}$$

and the time-bandwidth product is given by

$$\tau_p \Delta\nu_p = \frac{2\ln 2}{\pi}\sqrt{1+\left(\frac{b}{a}\right)^2} \approx 0.44\sqrt{1+\left(\frac{b}{a}\right)^2}. \tag{4.78}$$

For a Gaussian pulse without chirp this product will be given by $\tau_p \Delta f_p = 0.44$ and the pulse is thus **(Fourier) transform limited**. This shows that for the generation of ultra-short pulses laser media with broad gain spectra are necessary.

4.2.1 Active Mode Locking

In this section we derive how ultra-short pulses can be obtained by mode-locking of a laser, i.e. by generating a multi-longitudinal mode emission in which all the longitudinal modes are coupled in phase. This can be obtained by use of an intra-cavity frequency modulator such as an acousto- or electro-optic modulator, which induces a frequency shift on to the laser signal that corresponds exactly to the free-spectral range, and thus, the mode spacing of the cavity. Let us assume that the laser starts oscillating on the strongest line first, corresponding to a longitudinal mode index q_0. Then, after passing through the modulator, a fraction of the laser power will be shifted towards the modes $q_0 \pm 1$, that can be seen as sidebands to the main mode and which are also amplified, as the gain spectrum is assumed to be broad. As this shifted fraction usually has a much higher intensity than the spontaneous emission at that wavelength, the laser medium will predominantly amplify these shifted photons, which have a unique phase relation to the central mode q_0 with a phase difference ϕ. The amplified sidebands get shifted again, locking the modes $q_0 \pm 2$ to the central mode q_0 in phase with a phase difference 2ϕ. This scheme will go on until the shifted modes are outside of the amplification spectrum, as shown in Fig. 4.17. Therefore, an inhomogeneously broadened laser medium has to be used that provides gain for all the different longitudinal modes within its amplification spectrum.

To see that these locked modes correspond to a train of short pulses, we investigate the electric field of the laser emission [4]. For simplicity we assume that the locked modes are symmetrically distributed around the central mode q_0 and that they all have the same amplitude E_0. The electric field is then directly given by

$$E(t) = E_0 \sum_{k=-m}^{m} e^{2\pi i[(\nu_0 + k\Delta\nu_{FSR})t + k\phi]}. \tag{4.79}$$

As the cavity of length L is usually long compared with the length of the laser medium, the free spectral range can be approximated by

$$\nu_{FSR} = \frac{c}{2L}. \tag{4.80}$$

The summation in Eq. (4.79) can be performed analytically, resulting in an electric field

$$E(t) = A(t) e^{2\pi i \nu_0 t}, \tag{4.81}$$

with a time dependent amplitude

$$A(t) = E_0 \frac{\sin[(2m+1)\frac{2\pi\Delta\nu_{FSR}t + \phi}{2}]}{\sin[\frac{2\pi\Delta\nu_{FSR}t + \phi}{2}]}. \tag{4.82}$$

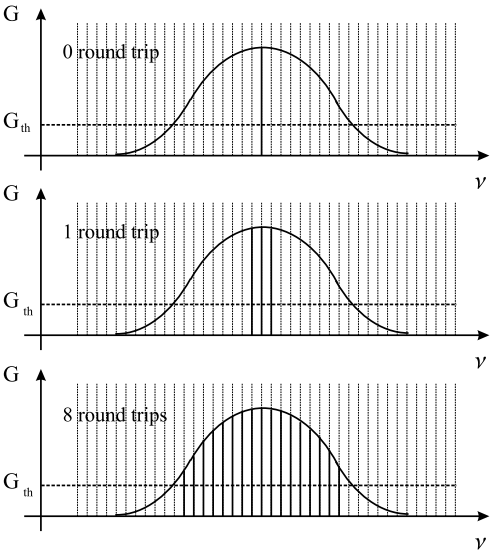

Fig. 4.17 Build-up of the longitudinal mode spectrum in a mode-locked laser after the laser emission started on the maximum gain line

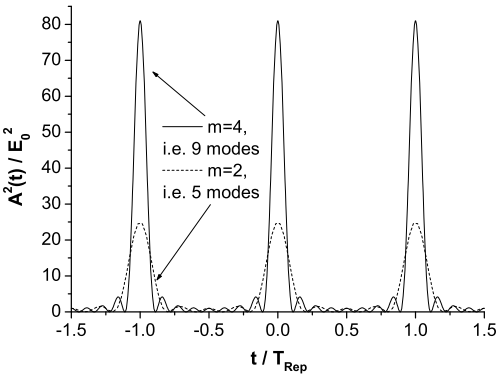

Fig. 4.18 Temporal pulse shape of phase-locked modes for two different values of m

The laser output intensity $I(t) \propto A^2(t)$ will therefore show an amplitude envelope on the high-frequency carrier oscillation ν_0 that corresponds to a train of pulses of width τ_p and a repetition period T_{Rep}, that can be seen in Fig. 4.18. The form of Eq. (4.82) is well known from a multi-slit interference experiment, in which the waves of the evenly spaced slits interfere after a certain distance on a screen. Here, this interference is not an interference in space, but in time, and the different slits correspond to the longitudinal modes that have a evenly distributed phase. The pulse maxima then occur at the times when the denominator in Eq. (4.82) is zero, which corresponds to a repetition rate

$$T_{Rep} = \frac{1}{\Delta\nu_{FSR}} = \frac{2L}{c}, \tag{4.83}$$

and which is just the round-trip time of the laser cavity. Therefore, this pulse train can also be seen as a single pulse with pulse width τ_p that circulates in the cavity. This pulse width can also be derived from Eq. (4.82), resulting in [4]

$$\tau_p \simeq \frac{1}{(2m+1)\Delta\nu_{FSR}}, \tag{4.84}$$

which will approach the inverse gain bandwidth of the laser medium under strong pumping, as then all modes may oscillate. As a result of the temporal interference of the different modes, the pulse peak power will be $(2m+1)^2$ times higher than for a laser in which the same modes are oscillating in an uncorrelated manner. Thus, mode-locking allows not only the generation of very short pulses, but also the generation of extremely high peak powers in the output beam.

An equivalent way of looking at the generation of mode-locked pulses is the case in which a loss is used as the frequency modulator in the cavity near to one of the cavity mirrors. This modulator is then driven by an external signal that causes a loss modulation with a frequency identical to the longitudinal mode spacing $\Delta\nu_{FSR}$. This amplitude modulation now causes the creation of sidebands, as discussed previously. An alternative view of this effect is the following: as the modulator causes loss minima at a frequency corresponding to the round-trip time of the resonator, the temporal evolution of the laser field that will have lowest loss is a short pulse that circulates inside the resonator and passes the modulator just at those times when the losses are low. The Fourier spectrum of this pulse can of-course only consist of several longitudinal cavity modes, and in order to create the pulse-like temporal evolution, they have to be locked in phase as shown in Eq. (4.79).

The first mode-locking of a laser used this type of loss modulation in a He-Ne laser in 1964. Pulses generated with this mode-locking technique usually are on the order of several ps.

4.2.2 Passive Mode Locking

As in passive Q-switching, the use of a saturable absorber in a laser cavity can also cause mode-locking. Therefore, the saturable absorber is placed just in front of the cavity end mirror. When the laser medium now is pumped the laser flux will start spiking as soon as the threshold of the cavity, including the absorber, is reached. This first intensity spike, which will circulate in the cavity with the round-trip time, saturates the absorber more than all other fluctuations of the growing laser field. It will, therefore, see the lowest round-trip loss and has thus maximum amplification and growth rate. As soon as this growing pulse dominates the inversion reduction, the laser will oscillate on a pulse train, which can again be described by Eq. (4.79). However, this point of operation, at which the saturable absorber has enough absorption to favor only one strong noise spike, can be difficult to achieve.

In a temporal scheme the saturable absorber will shorten the rise time of an incident pulse owing to the increasing transmission with increasing pulse intensity. The

amplifying laser medium itself creates the opposite process: as a result of the extraction of energy, and thus the reduction in gain, it will shorten the pulse by shortening the fall time of the pulse. However, in most solid-state lasers this effect is low compared with the shortening on the leading edge caused by the saturable absorber, as the upper-state lifetime is usually several orders of magnitude longer than the cavity round-trip time. The only case where both effects are dominant, is in the case of dye lasers, which show excitation lifetimes of the order of the cavity round-trip time. Therefore, ultra-short pulses on the fs-scale were mostly generated with dye lasers in the past.

Using special semiconductor quantum-well structures as saturable absorber and cavity mirror in one (SESAM), which exhibit a strong non-linear response, ultra-short pulses can also created with solid-state lasers. In this case, often a second mode-locking technique is used at the same time, to shorten the pulses further: this is Kerr-lens mode-locking.

Kerr-Lens Mode-Locking

A special way of passive mode-locking is Kerr-lens mode-locking (KLM), in which the self-focusing of an intense laser beam inside an optical medium is used. This effect is based on the Kerr-effect, the increase of the refractive index with increasing intensity $n(I) = n_0 + n_2 I$, and has a response time on the order of fs. In Kerr-lens mode-locking the laser medium is often used as the Kerr medium and an aperture is introduced into the cavity, either by insertion of a solid aperture or by a soft aperture, i.e. by the pumped volume. Assuming a parabolic intensity distribution inside the Kerr medium and a focal length much longer than the Kerr medium itself, it can be shown that the focal length of the Kerr lens is approximatively given by [3]

$$f_{Kerr} \approx \frac{w^2}{4 n_2 I_0 L}, \tag{4.85}$$

where, I_0 is the laser peak intensity, L the length of the Kerr medium and w the beam radius inside the Kerr medium. For a Ti:sapphire laser rod of $L = 4$ mm ($n_2 = 3.45 \times 10^{-16}\ \frac{\text{cm}^2}{\text{W}}$) and a 200 kW peak power beam focused to $w = 50$ µm, i.e. a peak intensity of

$$I_0 = \frac{P}{\pi w^2} = 2.5\ \frac{\text{GW}}{\text{cm}^2}, \tag{4.86}$$

we obtain a focal length of $f_{Kerr} \approx 18$ cm.

A Gaussian intensity distribution, e.g., thus exhibits a higher refractive index in its center compared with the wings of the radial intensity distribution. Hence, the Kerr medium acts as a positive lens and will focus the beam. Owing to the short response time, the strength of this focusing will be time dependent and only the temporally inner part of a laser pulse will see low losses at the aperture, as shown in Fig. 4.19. The leading and falling edge will be cut off, as their intensity is not sufficient to focus the beam through the aperture with low losses. In the case of a

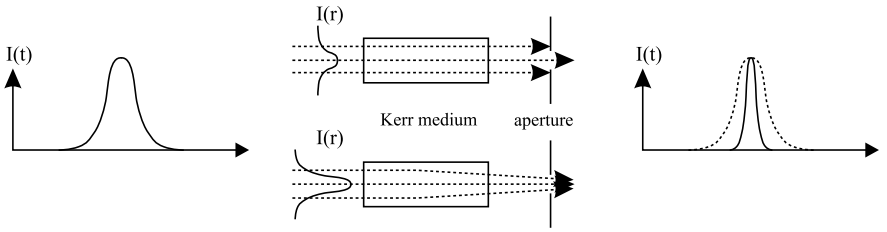

Fig. 4.19 Kerr-lens mode-locking

soft aperture, the focusing will increase the overlap between the beam and the pump volume, thus creating a higher gain for the high-intensity parts of the pulse, which also shortens the pulse. Using KLM in combination with a SESAM, it was possible to generate pulses of ~ 6.5 fs from a Ti:sapphire laser, a solid-state laser with a large gain bandwidth.

4.2.3 Pulse Compression of Ultra-Short Pulses

As already mentioned in Sect. 4.2, short pulses can exhibit a chirp. To understand how this chirp can build-up and how pulses can be compressed by reducing this chirp will be discussed in the following section. Therefore, we investigate the evolution of an incident laser pulse with an electric field amplitude of

$$E_i(t) = E_0 e^{-\xi_0 t^2} e^{i\omega_0 t} \tag{4.87}$$

propagating in a dispersive medium, where, the Gaussian parameter of the incident pulse is given by

$$\xi_0 = a_0 - i b_0. \tag{4.88}$$

The spectrum of this pulse is then expressed by

$$\tilde{E}_i(\omega) = \tilde{E}_0 e^{-\frac{(\omega-\omega_0)^2}{4\xi_0}}. \tag{4.89}$$

In a dispersive medium, the propagation constant $\beta(\omega)$ will show a non-linear dependence on ω, and can thus be approximated around the center frequency ω_0 by

$$\beta(\omega) \approx \beta_0 + \beta_1(\omega - \omega_0) + \beta_2(\omega - \omega_0)^2. \tag{4.90}$$

Thus, the spectrum of the pulse will change during the propagation according to

$$\tilde{E}(\omega, z) = \tilde{E}_i(\omega) e^{-i\beta(\omega)z}. \tag{4.91}$$

Using the Fourier transformation, this corresponds to a time dependence of the electric field of

$$E(t, z) = E_0 e^{i(\omega_0 t - \beta_0 z)} e^{-\xi(z)(t-\beta_1 z)^2}, \tag{4.92}$$

where, $\xi(z)$ is given by

$$\frac{1}{\xi(z)} = \frac{1}{\xi_0} + 2i\beta_2 z. \tag{4.93}$$

From Eq. (4.92) it can be seen that β_0 causes a propagation-distance-dependent phase delay as for any plane wave in a medium with an effective refractive index $n_{eff} > 1$, which can be expressed in terms of the **phase velocity**

$$v_{ph} = \frac{\omega_0}{\beta_0}. \tag{4.94}$$

In an optical medium with refractive index n, the phase velocity is given by $v_{ph} = \frac{c}{n}$ and $\beta_0 = k_z$ corresponds to the wave vector component in the propagation direction. However, in optical waveguides such as optical fibers the dispersion and index properties of the medium are changed resulting from the wave-guiding effect.

The influence of β_1 affects the Gaussian envelope of the electric field by introducing a delay on the envelope, which now propagates with the so-called **group velocity**

$$v_g = \left(\frac{\partial\beta}{\partial\omega}\right)^{-1}\Big|_{\omega=\omega_0} = \frac{1}{\beta_1}, \tag{4.95}$$

and the effect of β_2 is a change in the Gaussian parameter $\xi(z)$ with propagation distance, thus changing the shape of the pulse envelope, i.e. its pulse width and the chirp. As β_2 can be expressed as

$$\beta_2 = \left[\frac{\partial}{\partial\omega}\left(\frac{1}{v_g(\omega)}\right)\right]_{\omega=\omega_0}, \tag{4.96}$$

it is also called **group-velocity dispersion**. This influence on the pulse can be derived from Eq. (4.93), from which the real and imaginary part of the Gaussian parameter $\xi(z) = a(z) - ib(z)$ can be deduced as

$$a(z) = \frac{a_0}{(1+2\beta_2 b_0 z)^2 + (2\beta_2 a_0 z)^2}, \tag{4.97}$$

$$b(z) = \frac{b_0 + 2\beta_2 z(a_0^2 + b_0^2)}{(1+2\beta_2 b_0 z)^2 + (2\beta_2 a_0 z)^2}. \tag{4.98}$$

From Eqs. (4.97), (4.97), we can deduce why ultra-short pulses usually exhibit a chirp. Assuming a chirp-free Gaussian pulse, i.e. $b_0 = 0$, we find that by propagating this pulse in a dispersive medium, e.g. an output coupler mirror substate, vacuum windows or an optical fiber with non-zero group-velocity dispersion, it will exhibit an increasing chirp, which after a propagation length z in this medium is given by

$$b(z) = \frac{2\beta_2 z a_0^2}{1 + (2\beta_2 a_0 z)^2} = \frac{1}{2\beta_2}\frac{z}{z^2 + (\frac{\tau_p^2}{4\beta_2 \ln 2})^2}. \tag{4.99}$$

This chirp build-up is shown in Fig. 4.20, where, the reference length z_0 is given by

$$z_0 = \frac{\tau_p^2}{4\beta_2 \ln 2}. \tag{4.100}$$

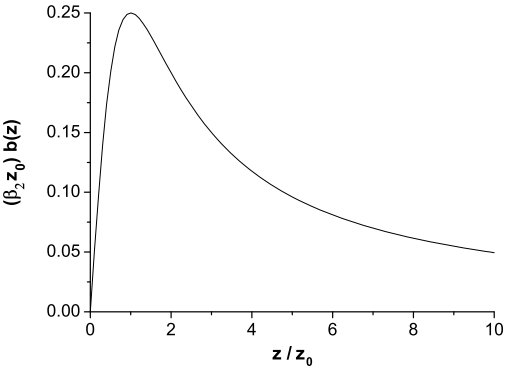

Fig. 4.20 Increasing chirp of an unchirped pulse propagating in a medium with group-velocity dispersion

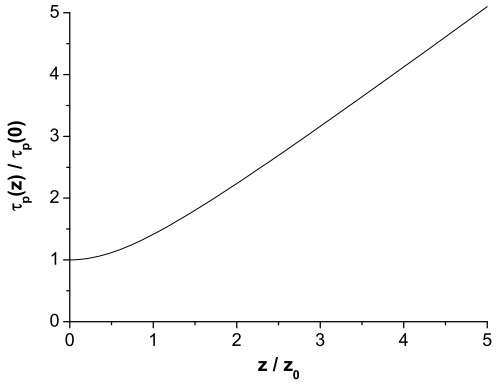

Fig. 4.21 Increasing pulse width of an unchirped pulse propagating in a medium with group-velocity dispersion

The pulse width then results in

$$\tau_p(z) = \tau_p(0)\sqrt{1 + \left(\frac{z}{z_0}\right)^2}, \tag{4.101}$$

a relation equivalent to the evolution of a the radial width of a Gaussian beam, see Eq. (3.44). Thus the incident pulse width will increase with propagation distance, as shown in Fig. 4.21.

However, as can also be seen from Eqs. (4.97), (4.98), a chirped pulse with incident chirp $b_0 \neq 0$ can be compressed in pulse width if a medium with proper group-velocity dispersion is used. The optimum group-velocity dispersion interaction length is given by

$$2\beta_2 L_{opt} = -\frac{b_0}{a_0^2 + b_0^2}, \tag{4.102}$$

which results in a maximum of $a(z)$ at $b(z) = 0$, and therefore, in a minumum pulse width

$$\tau_{p,min} = \frac{\tau_p(0)}{\sqrt{1 + (\frac{b_0}{a_0})^2}}. \tag{4.103}$$

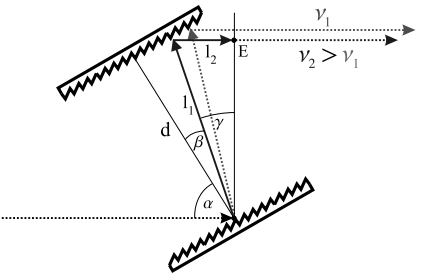

Fig. 4.22 Pulse compression using a pair of diffraction gratings

This corresponds to a pulse from which all chirp has been removed and transformed into its short pulse width. A large chirp will thus yield a high pulse width compression ratio with a final pulse that is Fourier transform limited when all chirp has been removed, as can be seen by inserting this result into Eq. (4.78).

Pulse Compression Methods

Depending on the actual chirp of the pulse, a medium or optical system with the proper group-velocity dispersion, is necessary in order to compress the pulse. Instead of using a massive medium with its natural dispersion, optical systems consisting of gratings or prisms are mostly used in these laser designs.

The grating design uses two diffraction gratings as shown in Fig. 4.22. Owing to the wavelength dependent diffraction angle, the internal optical path length of this grating system differs for different wavelengths, and will consequently create the necessary wavelength-dependent time delay to compress the pulse. Use of this technique enables large dispersion effects can be generated to compress pulses with strong chirps. The path length ΔL between the common incident point on the first grating and the point on the common exit plane of the grating compressor E, is given by

$$\Delta L = l_1 + l_2 = \frac{d}{\cos\beta} + \frac{d}{\cos\beta}\sin\gamma = \frac{d}{\cos\beta}(1+\sin\gamma). \tag{4.104}$$

Using the grating equation

$$\frac{\lambda}{g} = \sin\alpha - \sin\beta, \tag{4.105}$$

in which g is the grating period, the spatial dispersion is given by

$$\frac{\partial\Delta L}{\partial\lambda} = \frac{\partial\Delta L}{\partial\beta}\frac{\partial\beta}{\partial\lambda} = \frac{\lambda d}{g^2\cos^3\beta} = \frac{\lambda d}{g^2(1-(\sin\alpha-\frac{\lambda}{g})^2)^{\frac{3}{2}}}. \tag{4.106}$$

Therefore, the internal path length of the grating compressor will increase with wavelength, and will thus, create a larger time delay between the entry and exit planes for larger wavelengths. Hence, it will compress a pulse with a positive chirp.

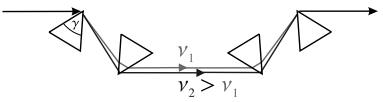

Fig. 4.23 Prism dispersion compensator for intracavity applications

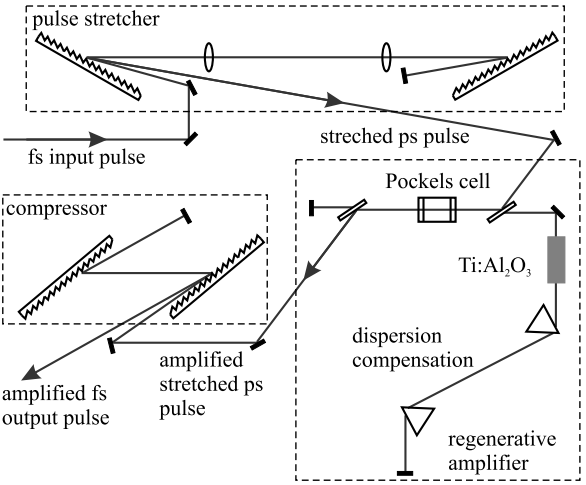

Fig. 4.24 Setup of a chirped-pulse amplifier, using gratings to stretch and compress the pulse and a prism pair for dispersion compensation [3]

A second alternative, which is mostly used to introduce a small correction to the cavity dispersion in a laser resonator for short-pulse mode-locking, is based on a system of prisms, which again shows a wavelength-dependent optical path length. In this case the prism material, as well as the geometry (prism angle γ), can be chosen so that the laser beam is incident on to the prism surfaces at Brewster's angle, for which the reflection losses are greatly reduced. The design in Fig. 4.23 also allows an easy insertion into an existing resonator, as the input and output beams are colinear. The strength of the dispersion introduced by this system, is lower than for a grating compressor; however, this prism compressor can be used to generate both signs of dispersion, i.e. either $\beta_2 < 0$ or $\beta_2 > 0$.

Chirped-Pulse Amplification

A main application of pulse compressors and its counterparts, pulse stretchers, is found in chirped-pulse amplification. This technique, depicted in Fig. 4.24, allows the generation of high-pulse-energy fs pulses. First, a standard fs mode-locked laser oscillator is used to generate fs pulses at a repetition rate of around 80 MHz with pulse energies on the order of some nJ. The oscillator pulses are then stretched in pulse width by passing an anti-parallel grating pair including a 1 : 1 telescope, creating a strong chirp on the pulse. Consequently, the pulse width is increased, e.g. by a factor of 3000 from 200 fs to 600 ps, decreasing enormously the pulse peak power. This now allows a high amplification of the pulses to pulse energies of several mJ without reaching the optical damage thresholds of the components in the amplifier.

The amplifier setup shown in Fig. 4.24 is a **regenerative amplifier**. The input pulses enter the amplifier by an intracavity polarizer. Then one pulse is selected by switching the Pockels cell to its half-wave voltage to rotate the polarisation of this pulse by 90°. It now passes the second polarizer and gets reflected by the cavity end mirror. At that time the Pockels cell is switched off. Thus the pulse keeps its polarisation and resonates back and forth in the amplifier cavity, where it passes a Ti:sapphire laser gain element twice for each round-trip.

In order to compensate for the internal cavity dispersion, a prism pair is also inserted into the amplifier cavity. When the pulse has made sufficient round-trips to reach its maximum pulse energy, the Pockels cell is switched to its half-wave voltage again while the pulse travels on the prism side of the cavity. Thus, when it comes back to the Pockels cell, it will be rotated by 90° and leaves the cavity by the second polarizer. Finally, the pulse chirp is removed in a grating compressor, reducing the pulse width back to the fs scale of the input pulse. Usually, the final pulse width is a bit longer than the original pulse width of the input pulse as a result of some additional higher-order chirp accumulated during the amplification steps. Whilst the damage threshold of the optical components in the stretched part of the setup are usually high enough, a critical point is the final grating of the compressor, at which the high-energy pulse has been compressed to its short pulse width, resulting in extreme peak powers. In order to prevent damage on that gratings, the beam diameter has to be strongly increased, making large-aperture gratings necessary.

References

1. A.E. Siegman, *Lasers* (University Science Books, Sausalito, 1986)
2. L.M. Frantz, J.S. Nodvik, J. Appl. Phys. **34**, 2346 (1963)
3. W. Koechner, *Solid-State Laser Engineering* (Springer, Berlin, 1999)
4. F.K. Kneubühl, M.W. Sigrist, *Laser* (Teubner, Stuttgart, 1999)